THE JOURNAL OF BIOLOGICAL CHEMISTRY VOL. 285, NO. 24, pp. 18939–18947, June 11, 2010

Canonical Wnt3a Modulates Intracellular Calcium and Enhances Excitatory Neurotransmission in Hippocampal Neurons*[S]

Received for publication, January 13, 2010, and in revised form, April 16, 2010 Published, JBC Papers in Press, April 19, 2010, DOI 10.1074/jbc.M110.103028

Miguel E. Avila[‡], Fernando J. Sepúlveda[§], Carlos F. Burgos[‡], Gustavo Moraga-Cid[§], Jorge Parodi[§], Randall T. Moon[¶1], Luis G. Aguayo[§], Carlos Opazo[§], and Giancarlo V. De Ferrari[‡‖2]

From the Departments of [‡]Biochemistry and Molecular Biology and [§]Physiology, Faculty of Biological Sciences, Universidad de Concepción, Concepción P.O. Box 4070386, Chile, [¶]Howard Hughes Medical Institute, Department of Pharmacology and Institute for Stem Cell and Regenerative Medicine, University of Washington School of Medicine, Seattle, Washington 98195, and the [‖]Center for Biomedical Research, Faculty of Biological Sciences and Faculty of Medicine, Universidad Andrés Bello, Santiago P.O. Box 8370134, Chile

A role for Wnt signal transduction in the development and maintenance of brain structures is widely acknowledged. Recent studies have suggested that Wnt signaling may be essential for synaptic plasticity and neurotransmission. However, the direct effect of a Wnt protein on synaptic transmission had not been demonstrated. Here we show that nanomolar concentrations of purified Wnt3a protein rapidly increase the frequency of miniature excitatory synaptic currents in embryonic rat hippocampal neurons through a mechanism involving a fast influx of calcium from the extracellular space, induction of post-translational modifications on the machinery involved in vesicle exocytosis in the presynaptic terminal leading to spontaneous Ca^{2+} transients. Our results identify the Wnt3a protein and a member of its complex receptor at the membrane, the low density lipoprotein receptor-related protein 6 (LRP6) coreceptor, as key molecules in neurotransmission modulation and suggest cross-talk between canonical and Wnt/Ca^{2+} signaling in central neurons.

Throughout mammalian brain development Wnt signaling seems to be spatially confined to specialized regions such as the olfactory bulb, frontal cortex, hippocampal formation, and the cerebellum (1–5). In these brain domains Wnt signaling has essential roles in diverse biological processes including neurogenesis (6), axonal remodeling (7), synapse formation, and maintenance of pre- and postsynaptic terminals (8–14). Indeed, several studies have begun to show that Wnt signaling may also be involved in excitatory synaptic transmission (15–18). For instance, activation of *N*-methyl-D-aspartate (NMDA)[3] receptors, after tetanic stimulation in rodent hippocampal slices, induces the release of a pool of vesicles containing Wnt3a in the synaptic terminal modulating long term potentiation events (18). Similarly, double-mutant mice for Wnt7a and Dishevelled-1, which exhibit decreases in the number of synapses between mossy fibers of the cerebellum and grainy cells, showed marked deterioration in the release of neurotransmitters and in the recycling of vesicles in the existing synapses (15). Furthermore, pharmacological analysis with drugs modulating Wnt signaling in hippocampal neurons showed an acute increase of neurotransmitters released from the presynaptic component, resulting in enhanced evoked basal activity and frequency of spontaneous and miniature excitatory currents (16). Finally, it has been reported that conditioned media containing canonical Wnt7a and to a lesser extent Wnt3a, but not conditioned media containing the noncanonical Wnt5a, which signals mainly through the Wnt/calcium (Wnt/Ca^{2+}) pathway (19, 20), were found to increase synaptic transmission in CA3-CA1 slices in adult rat hippocampus and to induce the recycling and exocytosis of synaptic vesicles in hippocampal neurons in culture (17).

Although these results indicate that Wnt signaling probably modulates neuronal transmission, the direct effect of a Wnt protein on synaptic transmission had not been demonstrated. Here we show that a purified Wnt ligand, the canonical Wnt/β-catenin Wnt3a protein, rapidly increased miniature synaptic currents through a mechanism involving Ca^{2+} mobilization and post-translational modifications on the machinery involved in vesicle exocytosis in the presynaptic terminal, suggesting cross-talk between canonical and Wnt/Ca^{2+} signaling in central neurons.

EXPERIMENTAL PROCEDURES

Wnt3a Purification—The Wnt3a purification was carried out following the protocol previously described (21), which has been implemented in our lab considering the changes sug-

* This work was supported by associative Comisión Nacional de Investigación Científica y Tecnológica Grant Programa Bicentenario en Ciencia y Tecnología ACT-04 from the Chilean government (to G. V. D., C. O., and L. G. A.).

[S] The on-line version of this article (available at http://www.jbc.org) contains supplemental Fig. S1.

[1] Supported as an Investigator of the Howard Hughes Medical Institute.

[2] To whom correspondence should be addressed: Center for Biomedical Research, Faculty of Biological Sciences and Faculty of Medicine, Universidad Andrés Bello, Santiago P.O. Box 8370134, Chile. E-mail: gdeferrari@unab.cl.

[3] The abbreviations used are: NMDA, *N*-methyl-D-aspartate; LRP, low density lipoprotein receptor-related protein; DIV, days *in vitro*; sFRP, secreted Frizzled-related protein; DKK, Dickkopf 1; ES, external solution; TTX, tetrodotoxin; CNQX, 6-cyano-7-nitroquinoxaline-2,3-dione; APV, D-2-amino-5-phosphonovaleric acid; ANOVA, analysis of variance; $GABA_A$, γ-aminobutyric acid, type A; Syp, synaptophysin; FM1-43, *N*-(3-triethylammoniumpropyl)-4-(4-(dibutylamino)styryl) pyridinium dibromide; AMPA, α-amino-3-hydroxyl-5-methyl-4-isoxazole-propionate.

gested by Kishida *et al.* (22). The presence of the Wnt3a protein was detected with an anti-Wnt3a antibody (R & D Systems, Minneapolis, MN), and the positive fractions were pooled and used in the next column. Purity was analyzed by SDS-PAGE (8%), stained with Coomassie Blue G250, and analyzed through densitometry by using software ImageJ.

Cultured Hippocampal Neurons—The animals were treated and handled according to National Institutes of Health guidelines. Hippocampal neurons were dissociated and maintained as described before (23). Briefly, the cells were taken from 18-day pregnant Sprague-Dawley rats and maintained for 12–13 days *in vitro* (DIV) on 35-mm tissue culture dishes with glass coverslips (350,000 cells/dish) coated with poly-L-lysine (Sigma). The neuronal feeding medium consisted of 80% minimal essential medium (Invitrogen), 10% heat-inactivated horse serum (Invitrogen), 10% heat-inactivated bovine fetal serum (Invitrogen), and a mixture of nutrient supplements. The culture was placed on a shelf in a 37 °C humidified CO_2 incubator, and the medium was changed every 3 days.

Wnt3a Functional Assays—Purified Wnt3a protein was assessed for its ability to stabilize β-catenin in hippocampal neurons (12–13 DIV), which were incubated with 10 nM of Wnt3a for 0 min, 15 min, 30 min, and 2 h. 10 mM LiCl (2 h; Sigma) was used as a control. Then the cells were lysed, and 30 μl of lysates were subjected to SDS-PAGE and Western blotting. Similarly, Wnt3a activity was evaluated in pBARL-HT22 cells, a mouse hippocampal cell line stably transfected with the pBARL (β-catenin-activated firefly luciferase) reporter plasmid, which contains 12 elements in response to T cell factor/lymphoid enhancer factor transcription factors (24). pBARL-HT22 neurons were incubated with different treatments, and after 24 h the luciferase activity was measured with a dual luminiscence kit (Promega, Madison, WI), as previously described (25), in a Victor3 multilabel counter (PerkinElmer Life Sciences). Recombinant secreted Frizzled-related protein 1 (sFRP1) and Dickkopf 1 (DKK1) were obtained from R & D Systems.

Electrophysiology—Whole cell patch clamp recordings were performed in 12–13 DIV hippocampal neurons as previously described (26, 27). Culture medium was changed to an external solution (ES) containing 150 mM NaCl, 5.0 mM KCl, 3.0 mM $CaCl_2$, 1.0 mM $MgCl_2$, 10 mM HEPES, and 10 mM glucose (pH 7.4, 330 mosmol). The patch pipette solution contained 120 mM CsCl, 4.0 mM $MgCl_2$, 10 mM 1,2-bis(*o*-aminophenoxy)ethane-*N*,*N*,*N*′,*N*′-tetraacetic acid, 10 mM HEPES, and 2 mM ATP (pH 7.35, 310 mosmol), and a holding potential of −60 mV was used. Stock recordings were obtained using an Axopatch-1D amplifier (Axon Instruments, Inc., Burlingame, CA). Electrodes were pulled from borosilicate capillary glass (WPI, Sarasota, FL) using a horizontal puller (Sutter Instruments, Novato, CA). The current signal was filtered at 2–5 kHz and stored for off-line analysis using personal computer interfaced with a Digidata 1200 acquisition board. In the records of action potentials, the current was set at 0 A. 100 nM tetrodotoxin (TTX) were added when miniature synaptic currents were recorded (2-min segments). Glutamatergic transmission was pharmacologically isolated during the recording of miniature synaptic currents through perfusion of Wnt3a in the presence of either 6-cyano-7-nitroquinoxaline-2,3-dione (CNQX; 4 μM) or D-2-amino-5-phosphonovaleric acid (APV; 50 μM), both of which were diluted in the ES without Mg^{2y+} for its preapplication at room temperature (20–24 °C; see Fig. 3). To obtain the mean average of either cumulative or peak amplitude and frequency, the data were analyzed with the Mini Analysis 6.0 program (Synaptosoft, Inc., Leonia, NY) as described previously (26). Decay time histograms were plotted with a bin of 1 pA, and the frequency (percentage of total events) was calculated and expressed over control neurons. All of the reagents were obtained from Sigma.

Calcium Experiments—Hippocampal neurons of 12–13 DIV were loaded with 5 μM Fluo-4AM (Molecular Probes and Invitrogen) in external solution for 30 min at 37 °C, washed three times with external solution for 5 min, and mounted in a perfusion chamber placed on the stage of an inverted fluorescent microscope (Eclipse TE, Nikon). The microscope had a 12-bit CCD camera attached (SensiCam, PCO, Germany). After being incubated for 15 min with different treatments (see "Results"), the neurons were located, selected by their somatic region, and illuminated (<0.266 s) by using a Lamba 10-2 filter wheel (Sutter Instruments) computer-controlled by Axon Instruments Work-Bench 2.2 software. The images at 480 nm were obtained at 2-s intervals during a continuous 5-min period, and the frequency of Ca^{2+} transients was determined. Because calcium transients are dependent on neuronal excitability and synaptic transmission and thus blocked by application of TTX (27, 28), Ca^{2+} transient records were performed in the absence of this inhibitor. Finally, a similar protocol was used when examining intracellular Ca^{2+} concentration, with the sole exception that this time the neurons were perfused with different treatments containing Wnt3a in the presence of inhibitors, and the images at 480 nm were obtained at 1-s intervals for a total recording period of 160 s.

Release of Synaptic Vesicles—Treated and control hippocampal neurons (10–13 DIV) were washed with ES and incubated for 5 min in high K^+ solution (30 mM) at 37 °C and then loaded with 15 μM probe FM1–43 (Molecular Probes) for 5 min at 37 °C, washed with ES for 5 min at room temperature, and mounted on a perfusion chamber. Different treatments were applied by perfusion (see "Results"), regions of interest were selected, and the decay of fluorescence associated with FM1–43 was continuously measured for 20 min. The recordings were collected with an inverted epifluorescence microscope (Eclipse TE; Nikon, Melville, NY) equipped with a Xenon lamp, 40× and 100× objectives, and a Lambda 10-2 filter wheel (Sutter Instruments). The microscope had a SensiCam CCD camera (PCO, Kelheim, Germany), and the FM1–43 fluorescence intensity was measured using a 2 × 2-pixel area. FM1–43 was excited at 560 nm, and emission was collected with a 620-nm filter. Finally, a similar approach was used when loading for 1 min neurons with 50 μM of the fixable probe AM1–43 (Molecular Probes) at 37 °C, after which the cells were washed with ES for 5 min at room temperature and mounted on a perfusion chamber for immunocytochemistry.

Immunocytochemistry—Treated and control hippocampal neurons (10–13 DIV) were washed with ES and loaded with 50 μM AM1–43 (Molecular Probes) for 1 min at 37 °C, washed

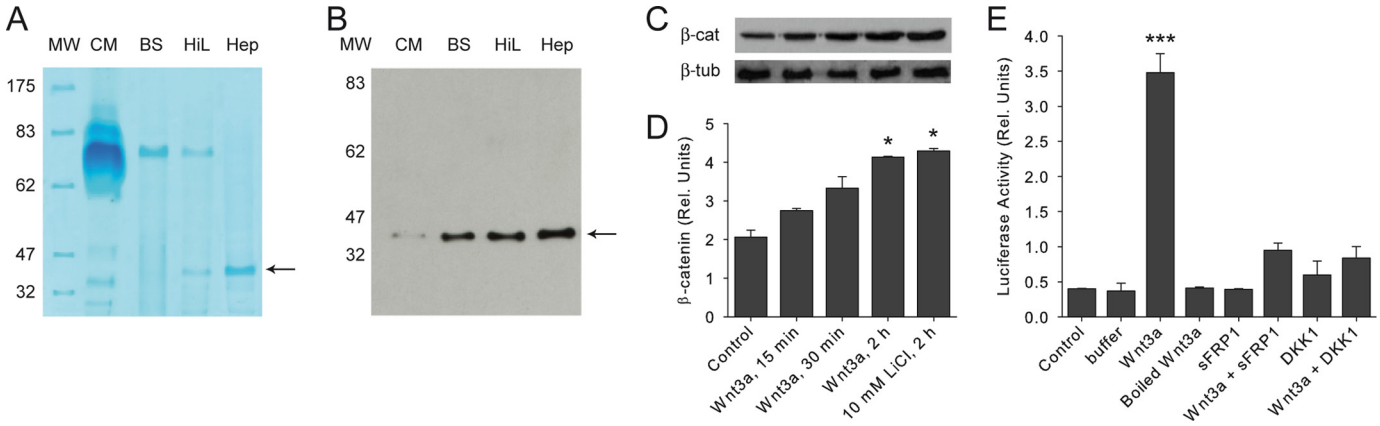

FIGURE 1. **Purification and functional assays of Wnt3a activity.** *A*, Coomassie Blue staining of an SDS-PAGE gel that was loaded with Wnt3a L-cell conditioned medium (*CM*) and purified Wnt3a, resulting from a three-step chromatographic purification. *BS*, Blue Sepharose; *HiL*, High Load 16–60 Superdex 200; *Hep*, heparin; *MW*, molecular mass. *B* and *C*, Western blotting analysis of purified Wnt3a and time-dependent effect on β-catenin stabilization in hippocampal neurons following different periods of Wnt3a application (15 min, 30 min, and 2 h); LiCl (10 mM) for 2 h was used as a control. *D*, summary of data as shown in *C*. *E*, β-catenin reporter activity in pBARL-HT22 cells treated with 10 nM Wnt3a, Wnt3a vehicle (*buffer*), boiled Wnt3a (denatured 10 min at 96 °C), 10 nM Wnt3a plus 50 nM recombinant sFRP1, 50 nM sFRP1, Wnt3a plus 70 nM recombinant DKK1, and 70 nM DKK1. *Control*, basal reporter activity in this cell line. The data from three independent experiments are shown as the means ± S.E., and test ANOVA (*, $p < 0.05$; ***, $p < 0.005$) was implemented.

with ES for 5 min at room temperature, and mounted on a perfusion chamber. The cells were fixed with 4% paraformaldehyde + 1× phosphate-buffered saline (pH 7.4), blocked for 1 h with horse fetal serum (1:10 Hyclone), permeabilized with 1× phosphate-buffered saline + Triton X-100 (0.1%), and incubated for 12 h at 4 °C with the following primary antibodies: p-Synapsin I antibody (Ser-553; 1:200; Santa Cruz Biotechnology, Santa Cruz, CA), LRP6 (1:100; R & D Systems), synaptophysin (1:500; Zymed Laboratories Inc.), and PSD95 (1:500; Affinity Bioreagent). Then the neurons were washed three times and incubated with the appropriate secondary antibodies conjugated to Alexa488 (1:500), Cy3 (1:400), and Alexa633 (1:500) (Jackson ImmunoResearch Laboratories). After mounting the samples in Dako (Dako Corp.), fluorescent microscopy was performed (60 × oil immersion objective, 1.45 NA) using a TE2000U confocal microscope (Nikon). The images were acquired with the Nikon software EZ-C1 version 3.5.

Colocalization Analysis—Fluorescent images for each antibody were acquired sequentially on the confocal microscope. We selected regions of interest (neuronal process) adjusted to a window/level of 300 pixels and separated the fluorescence channels associated with LRP6, synaptophysin (Syp), and PSD95. The images were deconvoluted and examined for the degree of colocalization between the different channels through qualitative analysis of antibody colocalization using ImageJ (plug-in JacoP). Overlap of the green-red (LRP6-Syp) and green-blue (LRP6-PSD95) channels were visualized in merged images, and then overlapping areas were considered as colocalized. The extent of colocalization was further analyzed using the Mander's (M1) and Pearson's coefficients (29). Both coefficients range from 0 to 1, with 0 indicating low colocalization and 1 indicating high colocalization.

Western Blot—The proteins were separated in a SDS-PAGE 12% gel and transferred to a nitrocellulose membrane (Bio-Rad). The membranes were blocked with 5% milk in 1× phosphate-buffered saline and 0.1% Tween 20 for 1 h in agitation, then incubated with primary β-catenin or p-Synapsin I (Ser-553) antibodies (both from Santa Cruz Biotechnology) for 12 h at 4 °C, washed, and incubated with appropriate secondary antibody conjugated to horseradish peroxidase (Santa Cruz Biotechnology) for 1 h at 4 °C. The immunoreactivity of reactive protein was detected using chemoluminescence reagents (Promega).

Data Analysis—The data are shown as the means ± S.E. and test ANOVA (*, $p < 0.05$; **, $p < 0.01$; ***, $p < 0.005$) was implemented. All of the analyses were performed using Origin 6.0 software (Microcal, Inc., Northampton, MA).

RESULTS

Purified Wnt3a Enhances Excitatory Neurotransmission—We purified Wnt3a protein from stable mouse L-cells following standard protocols (21, 22) and consistently recovered a fully functional Wnt3a ligand that induced accumulation of its β-catenin target in primary cultures of embryonic rat hippocampal neurons (12–13 DIV) (Fig. 1, *A–D*). Then to analyze the functional activity of the Wnt3a protein in mature synapses in hippocampal neurons, we carried out electrophysiological analysis using the whole cell patch clamp technique to record spontaneous synaptic activity in the presence of different concentrations of the purified protein. We found that Wnt3a produced a concentration-dependent increase in the frequency of spontaneous synaptic currents (Fig. 2*A*), which at the cellular level is likely associated with an increase in the activity of the neuronal network, reflecting the sum of action potentials and synaptic potentials. Analyses of characteristic parameters of action potentials (*i.e.* threshold, amplitude, and duration) showed that no significant differences were found in control *versus* treated neurons with 10 nM Wnt3a for 15 min (Fig. 2*B* and Table 1). Interestingly, although individual action potentials remained similar, there was a greater number of repetitive events in Wnt3a-treated neurons (Fig. 2*B*, *bottom trace*), reflecting an increase of the neural network excitability and further indicating that the effect of the Wnt3a protein ought to be mainly on synaptic transmission (increased synaptic potential). Moreover, there were no significant differences in input resistance in control and Wnt3a-treated neurons (Table 1).

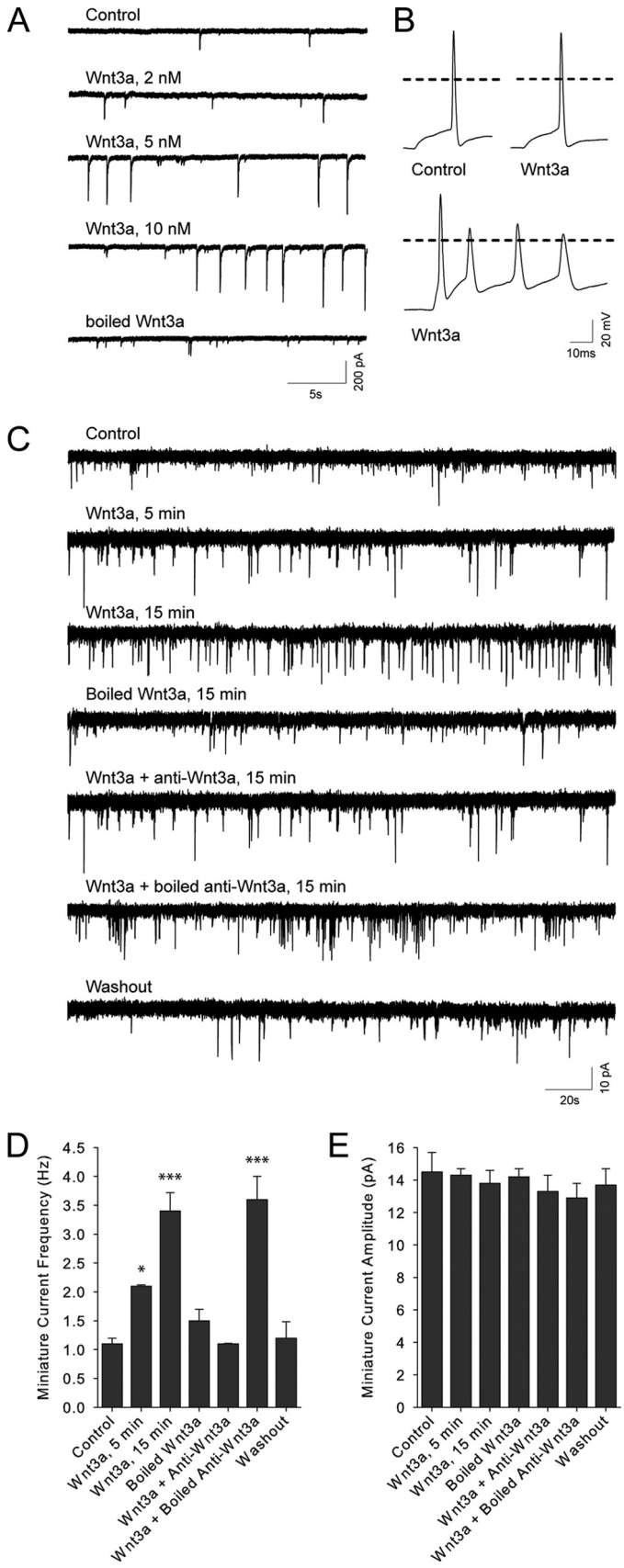

FIGURE 2. **Enhancement of miniature synaptic activity by purified Wnt3a in primary cultures of hippocampal neurons.** *A*, representative traces of spontaneous synaptic currents recorded in the presence of different Wnt3a concentrations (0–10 nM). *B*, the *upper panel* shows representative traces of individual events in voltage records (action potentials) obtained from control neurons and those treated with 10 nM of the Wnt3a protein. The *lower panel* depicts a repetitive event induced by 10 nM Wnt3a. The *dotted lines* mark 0 mV. The records ($n = 5$) were obtained in the absence of TTX, and the treatments were applied by perfusion. *C*, miniature synaptic activity following the application of Wnt3a (5 and 15 min) and various treatments by perfusion in the presence of 100 nM TTX (holding potential of −60 mV; 2-min duration). *D* and *E*, summary of miniature synaptic activity data for current frequency and amplitude, respectively. *Control*, Wnt3a vehicle; *Wnt3a*, 10 nM Wnt3a; *Boiled*, denatured Wnt3a (boiled 96 °C); *anti-Wnt3a*, antibody anti-Wnt3a; *Boiled anti-Wnt3a*, boiled antibody anti-Wnt3a (96 °C); *washout*, Wnt3a removed from external solution. Test ANOVA was implemented (***, $p < 0.005$; $n = 5$). The data are shown as the means ± S.E.

TABLE 1

Electrical parameters (action potentials and input resistance) recorded in hippocampal neurons in the absence or presence of Wnt3a (10 nM , 15 min)

AMP, amplitude; TH, threshold; AP/2, duration of action potentials; IR, input resistance.

	Action potential			IR
	AMP	TH	AP/2	
	mV	*mV*	*ms*	*GΩ*
Control	84 ± 1.4	−46 ± 0.6	$0.0015 \pm 5.0 \times 10^{-5}$	0.65 ± 0.05
Wnt3a	85 ± 1.5	−44 ± 1.0	$0.0014 \pm 7.3 \times 10^{-5}$	0.7 ± 0.04
p value	0.56	0.13	0.45	0.32

Thus, we decided to use 10 nM of Wnt3a as the effective concentration for subsequent recordings of synaptic potentials (miniature synaptic activity), examined in the presence of 100 nM of the Na^+ channel blocker TTX.

Local application of Wnt3a to neurons showed a time-dependent enhancement of miniature synaptic activity compared with control neurons treated with the Wnt3a elution buffer (Fig. 2*C*). Analysis of individual traces (*i.e.* mean average peak) revealed that purified Wnt3a significantly affected the frequency but not the amplitude of the synaptic currents (Fig. 2, *C–E*), an effect that was further confirmed by analyses of the cumulative frequency and amplitude between control and Wnt3a-treated neurons (supplemental Fig. S1). The enhancing effect on frequency was apparent after 5 min and peaked at 15 min of incubation (1.1 ± 0.1 Hz in control conditions to 3.4 ± 0.3 Hz in the Wnt3a treatment; $n = 9$), and contrary to Wnt3a-treated neurons, either the application of denatured Wnt3a (1.5 ± 0.2 Hz; $n = 8$) or the coapplication of 2 μg/ml of anti-Wnt3a antibody (1.1 ± 0.01 Hz; $n = 8$), at a dose that blocks Wnt3a activity in Wnt/β-catenin reporter-based luciferase assays (Fig. 1*E*), was without effects on synaptic activity. Conversely, the inhibitory effect of the anti-Wnt3a antibody was not observed when this antibody was previously denatured (3.6 ± 0.4 Hz; $n = 5$). Moreover, the effect of Wnt3a was reversible as demonstrated after its removal from the bath solution (washout; 1.2 ± 0.5 Hz; $n = 9$; Fig. 2).

Wnt3a-mediated enhancement in the frequency of miniature synaptic currents was completely blocked in the presence of CNQX (4 μM), an inhibitor of AMPA receptors (0.7 ± 0.1 Hz; $n = 5$), and partially silenced in the presence of APV (50 μM), a competitive antagonist of NMDA receptors (0.9 ± 0.1 Hz; $n = 5$), suggesting that modulation of excitatory glutamatergic neurotransmission plays a fundamental role in the synaptic effect induced by Wnt3a (Fig. 3, *A* and *B*). As previously observed, the amplitude of synaptic currents did not differ among treatments

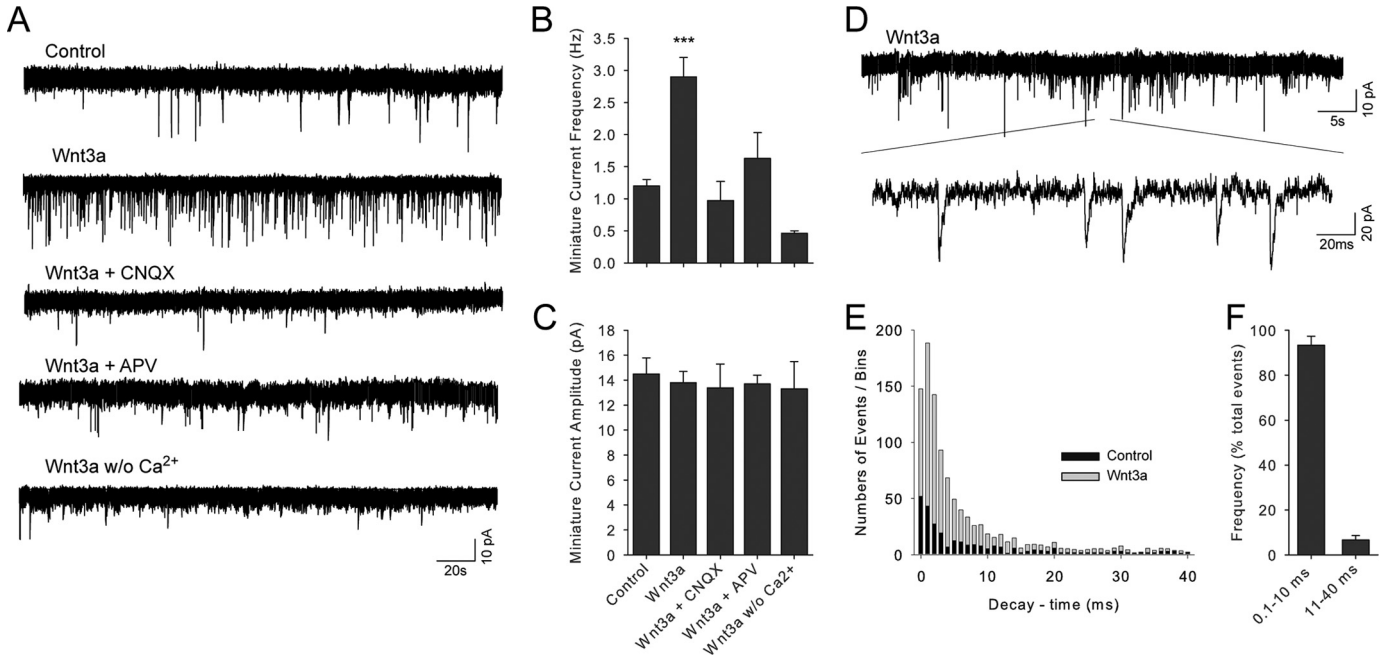

FIGURE 3. **Inhibition of Wnt3a-induced synaptic activity by glutamatergic blockers CNQX and APV.** *A*, the miniature synaptic transmission induced by 10 nM Wnt3a (15 min) in hippocampal neurons was pharmacologically blocked following application of CNQX (4 μM) or APV (50 μM) by perfusion in the presence of ligand and TTX (100 nM) and in the absence of Mg^{2+}. *B* and *C*, data summary for the effects on the frequency and amplitude of the miniature currents, respectively. *Control*, Wnt3a vehicle; *w/o* Ca^{2+}, zero nominal calcium. The data are shown as the means ± S.E., and test ANOVA (*, $p < 0.05$; ***, $p < 0.005$; $n = 5$) was implemented. *D–F*, analysis of an extended trace of miniature synaptic activity recorded in the presence of 10 nM Wnt3a. *E* and *F*, stacked bars plot showing event decay-time (ms) distribution histogram and the frequency of total events in Wnt3a-treated neurons. *0.1–10 ms*, fast AMPAergic events; *10–40 ms*, slow GABAergic events.

(Fig. 3*C*). Furthermore, analysis of time decay kinetics of synaptic events (26, 27) showed that records in the presence of Wnt3a were easily distinguishable as glutamatergic, specifically AMPAergics (93%; $\tau = 0.1–10$ ms; $n = 10$), in contrast to NMDA/GABAergic kinetics (7%; $\tau = 11–40$ ms; $n = 9$) (Fig. 3, *D–F*). Therefore, we conclude that low concentrations of purified Wnt3a rapidly enhance the frequency of miniature excitatory synaptic currents and that such an effect is specific to treatments with the purified Wnt3a protein.

Wnt3a Induces Intracellular Ca^{2+} Influx and the Release of Presynaptic Vesicles—Changes in the frequency of miniature synaptic currents could be interpreted by alterations in the probability of neurotransmitter release, and it has been suggested that such release depends on the concentration of Ca^{2+} within the presynaptic terminal (30). Interestingly, the effect of Wnt3a on the frequency of miniature synaptic activity was completely abolished (0.5 ± 0.05 Hz; $n = 5$) when an external solution with zero nominal Ca^{2+} was used in the experiments (Fig. 3, *A–C*). Therefore, we next investigated whether there was a relationship between the Wnt3a-induced enhancement in excitatory synaptic transmission and intracellular Ca^{2+} levels. To do so, neurons were loaded with Fluo4-AM, and the fluorescent signal related to the frequency of spontaneous calcium transients was recorded using fluorescence microscopy. Notably, as shown in Fig. 4*A*, neurons incubated with a concentration of 10 nM Wnt3a for 15 min and in the absence of TTX significantly augmented the frequency of spontaneous Ca^{2+} transients ($13.9 \pm 0.5 \times 10^{-2}$ Hz; $n = 50$) when compared with control cells ($3.6 \pm 0.1 \times 10^{-2}$ Hz; $n = 45$, $p < 0.005$). Conversely, neurons treated either with denatured Wnt3a (boiled) or coincubated with Wnt3a and anti-Wnt3a (2 μg/ml) did not show the above mentioned effect ($4.1 \pm 0.2 \times 10^{-2}$ and $4.7 \pm 0.6 \times 10^{-2}$ Hz, respectively). As a way to distinguish among the Ca^{2+} source required for the synaptic effect of the Wnt3a protein, we next examined whether acute perfusion of Wnt3a altered intracellular Ca^{2+} levels using the fluorescent probe Fluo4-AM (Fig. 4*B*). Consistent with our previous results, perfusion of Wnt3a acutely augmented the intracellular Ca^{2+} concentration of neurons loaded with Fluo4-AM, an effect that was partially reversed when Wnt3a was coincubated with 2 μg/ml of the anti-Wnt3a antibody (decreased to 46% of the Wnt3a normalized fluorescence signal, $n = 15$) or silenced when a denatured fraction of purified Wnt3a was used after being heated for 10 min at 96 °C (decreased to 8% of normalized fluorescence, $n = 6$). Remarkably, the Wnt3a effect on intracellular Ca^{2+} was dramatically diminished in the presence of 20 μM Cd^{2+} (12.2 ± 0.8% of the Wnt3a normalized signal, $n = 15$), which acts as a nonselective Ca^{2+} channel blocker, and nearly abolished in the absence of extracellular calcium in the working solution (zero nominal calcium; 3.7 ± 1.1% of the remaining signal, $n = 18$), thus indicating that the extracellular space is the main source of the Ca^{2+} mobilized by the Wnt3a ligand.

It has been proposed that intracellular Ca^{2+} concentration is the focal point controlling the exocytosis and trafficking of synaptic vesicles at the presynaptic active zone of nerve terminals (31). Therefore, to examine whether the effect of Wnt3a on the intracellular Ca^{2+} concentration was sufficient to allow the release of presynaptic vesicles from mature hippocampal neurons, we applied a depolarizing stimulus with a high K^+ concentration (30 mM) and loaded neurons with FM1–43, and then

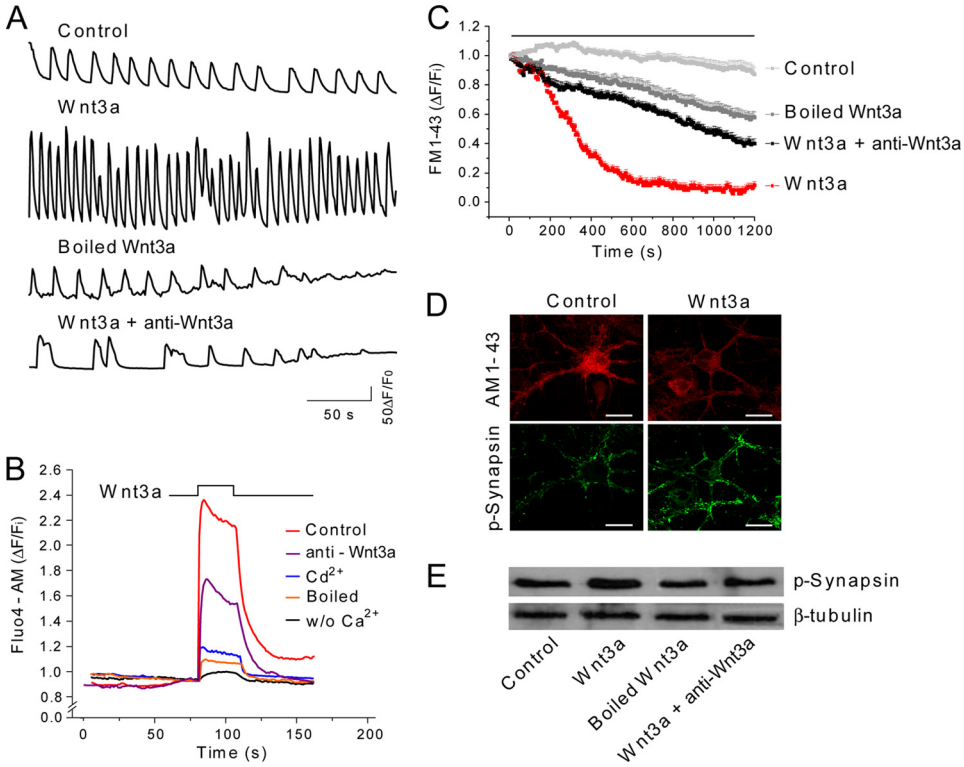

FIGURE 4. **Enhancement of intracellular Ca^{2+} and synaptic vesicle release by Wnt3a in hippocampal neurons.** *A*, representative fluorescent traces showing spontaneous enhancement of calcium transients following application of Wnt3a and various treatments for 15 min. *B*, strokes representing the effect of acute influx of extracellular Ca^{2+} following perfusion of Wnt3a and various treatments. *C* and *D*, synaptic vesicle release from presynaptic terminals induced by Wnt3a. *C*, destaining associated to FM1–43 (depleted fraction, $\Delta F/F_i$) in the presence or absence of Wnt3a. Treatments were applied by perfusion during the entire record (20 min), and the burden of hippocampal neurons was recorded ($n = 60–80$ neurons). *D*, immunocytochemical analysis showing the decay of the signal associated with the fixable AM1–43 probe (*upper panels*) and the enhancement of phosphorylated Synapsin I (Ser-553) after treatment with Wnt3a for 15 min (*lower panels*). The *calibration bar* represents 20 μm. *E*, Western blot of phosphorylated Synapsin I after treatment for 15 min with purified Wnt3a compared with control neurons either treated with boiled Wnt3a or coincubated with a Wnt3a-specific antibody. All records of Ca^{2+} changes were made in the absence of TTX. *Control*, Wnt3a vehicle; *ENS*, external normal solution containing 10 nM Wnt3a; *Cd^{2+}*, ENS plus 10 nM Wnt3a and 20 μM Cd^{2+}; *w/o Ca^{2+}*, 10 nM Wnt3a plus external solution without Ca^{2+} (zero nominal Ca^{2+}); *Boiled*, denatured Wnt3a (boiled 10 min to 96 °C); *anti-Wnt3a*, coincubation of 10 nM Wnt3a and 2 μg/ml of antibody anti-Wnt3a.

treatments (*i.e.* Wnt3a) were applied by perfusion throughout the entire record (Fig. 4*C*). Indeed, time course experiments revealed that Wnt3a treatment induced a fast release of synaptic vesicles seen as the decay in the fluorescence associated with FM1–43 after starting the incubation, which subsequently reached a plateau at 12–15 min of stimulation (Fig. 4*C*). The value of the depleted fraction ($\Delta F/F_i$) found after 20 min of recording was 0.1 ± 0.04 in the control condition and 0.8 ± 0.02 in neurons treated with Wnt3a. Similarly, such an effect was specific to Wnt3a because no significant differences were observed when boiled Wnt3a and coincubation with the anti-Wnt3a antibody were used as treatments (0.42 ± 0.03 and 0.6 ± 0.03, respectively). In agreement with the above presented results, fluorescent immunochemistry analysis in hippocampal neurons with the fluorescent probe AM1–43 (equivalent dye to FM1–43 but with the additional property of being fixable) showed that the signal associated with synaptic vesicles strongly decreased after 15 min of treatment with purified Wnt3a (Fig. 4*D*, *upper panels*). Collectively, these experiments, which were made in the absence of TTX, indicate that acute incubations with purified Wnt3a allows the influx of Ca^{2+} from the extracellular space, augmenting the intracellular concentration of Ca^{2+} and enhancing the release of synaptic vesicles from the presynaptic terminal.

Previous studies have shown that Wnt-7a induced the clustering at remodeled areas of mossy fibers of the neuron-specific phosphoprotein Synapsin I as a preliminary step in synaptogenesis (11). Therefore, we further investigated whether Wnt3a treatment had any effect on such post-translational modification in hippocampal neurons. Indeed, purified Wnt3a induced a substantial increase in the signal of phosphorylated Synapsin I (shown in *green*) when compared with control neurons (Fig. 4*D*, *lower panels*). Finally, Western blot analysis revealed that induction of Synapsin I phosphorylation was specific for the treatment with purified Wnt3a (Fig. 4*E*), suggesting that this post-translational modification may be an essential step toward the release of synaptic vesicles from presynaptic terminals induced by Wnt3a in hippocampal neurons.

Involvement of the Wnt/β-Catenin Complex Receptor at the Membrane in Wnt3a Neurotransmission—As shown previously, purified Wnt3a induced β-catenin accumulation in hippocampal neurons (Fig. 1, *C* and *D*). Then would the molecular machinery normally transducing canonical Wnt3a be the one responsible for the enhancement of intracellular calcium and the fast release of synaptic vesicles from the presynaptic terminals? We began to approach this question by interfering with Wnt3a signal presentation at the membrane using recombinant proteins that inhibit the activity of its complex receptor Frizzled-LRP5/6. Therefore, the synaptic activity of hippocampal neurons exposed to Wnt3a was recorded either in the presence of 50 nM sFRP1, a Wnt antagonist, or in the presence 2 μg/ml DKK1, an antagonist of LRP6 that acts as a coreceptor (32). Remarkably, we observed blockade of the Wnt3a effect by both sFRP1 and DKK1 on the frequency of miniature synaptic currents (1.6 ± 0.14 Hz, $n = 6$ and 1.2 ± 0.04 Hz, $n = 5$, respectively; Fig. 5*A*) and Ca^{2+} transients ($3.8 \pm 0.4 \times 10^{-2}$ Hz, $n = 40$ and $6.8 \pm 0.09 \times 10^{-2}$ Hz, $n = 50$, respectively; Fig. 5*B*), suggesting that the Wnt/β-catenin complex receptor is functionally active at the synaptic terminal. No significant increase was observed when sFRP1 and DKK1 proteins were applied alone onto the hippocampal neurons.

DKK1 interferes directly with Wnt3a presentation to the LRP6 receptor itself, instead of being sequestered in the extra-

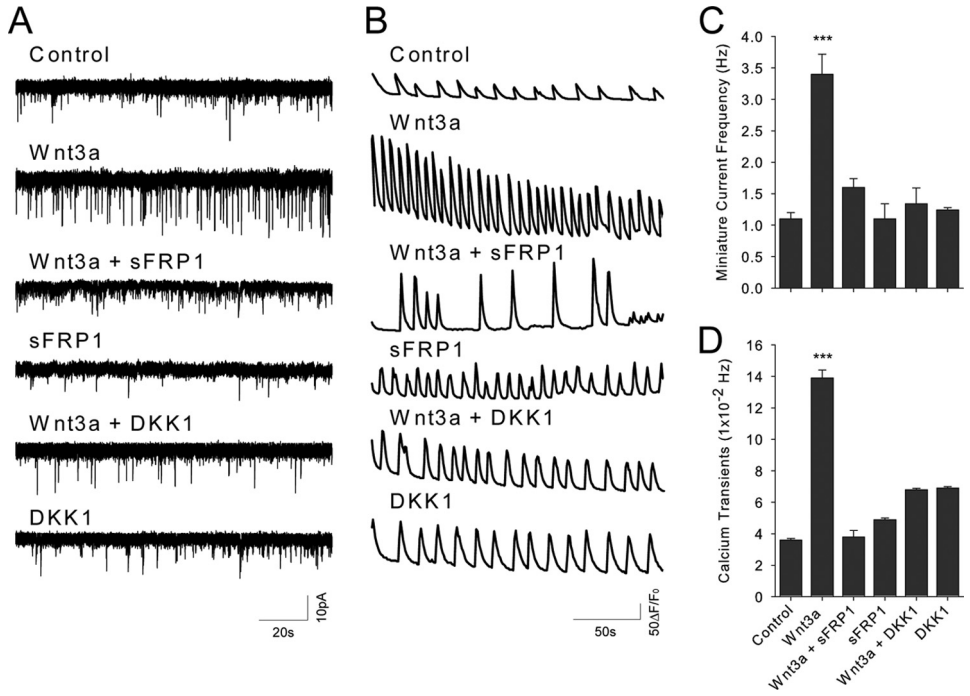

FIGURE 5. **Evidence for the participation of the Wnt/β-catenin complex receptor in Wnt3a-induced neurotransmission.** *A* and *B*, representative traces showing the inhibition of the Wnt3a enhancement in the frequency of miniature synaptic activity (test ANOVA; ***, $p < 0.005$; $n = 5$; 100 nM TTX) and calcium transients (test ANOVA; ***, $p < 0.005$; $n = 40–50$), respectively, following coincubation for 15 min of 10 nM Wnt3a with either 50 nM sFRP1 or 70 nM DKK1, which act as inhibitors of the Wnt/β-catenin membrane-associated receptors (see also Fig. 1*E*). *C* and *D*, summary of miniature synaptic activity frequency and calcium transient data, respectively. The data are shown as the means ± S.E.

cellular space as is the case for the action of sFRP1. Given that we have previously shown that the LRP6 protein is expressed in the human hippocampus (25), we wanted to study whether LRP6 was present in the synaptic terminal. To do so, the subcellular localization of the LRP6, as well as pre- and postsynaptic markers Syp and PSD95, respectively, was examined in 14–15 DIV hippocampal neurons by confocal microscopy. The results obtained are summarized in Fig. 6, which shows that LRP6 is widely distributed both in the soma and in the neuronal processes of hippocampal neurons, where it is colocalized and/or closely apposed to the signal corresponding to synaptophysin and PSD95. Further quantitative analysis of colocalization for LRP6-Syp and LRP6-PSD95 proteins (Fig. 6, *B* and *C*) revealed that there were no significant differences in the colocalization coefficients, Mander's (0.34 ± 0.042 and 0.38 ± 0.044, respectively; $n = 15$) or Pearson's (0.54 ± 0.029 and 0.52 ± 0.027, respectively; $n = 15$) (29), suggesting that the LRP6 could be simultaneously present in both pre- and postsynaptic terminals.

DISCUSSION

In recent years it has become clear that the signaling cascade activated by any Wnt isoform is highly dependent on cellular context or the complementation between cell surface Wnt receptors (33). Wnt3a belongs to the so-called Wnt/β-catenin or canonical signaling as opposed to the β-catenin-independent or noncanonical pathways, which transduce their signals to control asymmetric cell division and morphogenetic movements during vertebrate gastrulation, including the Wnt/Ca^{2+} pathway (19, 20, 32). Here we demonstrate that synaptic transmission activity was modulated by direct application of a canonical Wnt3a protein to mature hippocampal neurons, which is in general agreement with the effect of a recombinant Wnt3a preparation used to study long term potentiation events on hippocampal slices (18) and the use of either conditioned medium containing Wnt ligands (15, 17) or Wnt/β-catenin small molecule modulators (16). Moreover, the effect was dependent on the incubation with the purified protein (Figs. 2–4) and not observed in the presence of recombinant DKK1 and sFRP1 proteins, classical inhibitors of the Wnt/β-catenin pathway (Fig. 5), suggesting that the canonical complex receptor at the membrane is functionally active at the synaptic terminal.

Although we initially observed that purified Wnt3a induced an increase both in the frequency and the amplitude of spontaneous activity in Wnt3a-treated neurons (Fig. 2*A*), which could reflect enhanced neuronal excitability, we subsequently observed that the Wnt3a-dependent effect was not due to changes in neuronal electrical parameters such as action potentials or input resistance (Fig. 2*B* and Table 1). Moreover, analyses of miniature postsynaptic currents in TTX-treated neurons indicate that the Wnt3a effect was directly on synaptic transmission, via augmenting the frequency of neurotransmitter release, and not related to the number of activated receptors in the postsynaptic region (Fig. 2, *C–E*; see also supplemental Fig. S1).

To investigate whether excitatory or inhibitory neurotransmission is the target of purified Wnt3a, we first evaluated the effects of excitatory AMPA/kainate and NMDA receptors. Our results show that when neurons were treated with 4 μM CNQX (AMPA/kainate antagonist), the Wnt3a effect on the release of synaptic vesicles was dramatically decreased (*i.e.* similar to that observed in the control neurons) (Fig. 3, *A-C*). Similarly, in the case of the NMDA receptor antagonist APV, the results show that although there was not complete inhibition, no significant differences were observed between APV-treated and control neurons. Finally, considering that the blockade of $GABA_A$ receptors with bicuculline or strychnine induced an increase in the frequency of miniature AMPA receptor-mediated postsynaptic currents (34) and a change in the network activity of hippocampal neurons (27, 34), which were within the time frame for the Wnt3a effect described here (*i.e.* > 15 min), as an indirect way to assess the effects on inhibitory activity, we carried out analyses of time decay kinetics (τ) events. In agreement with previous observations (15–18), our results clearly distinguished

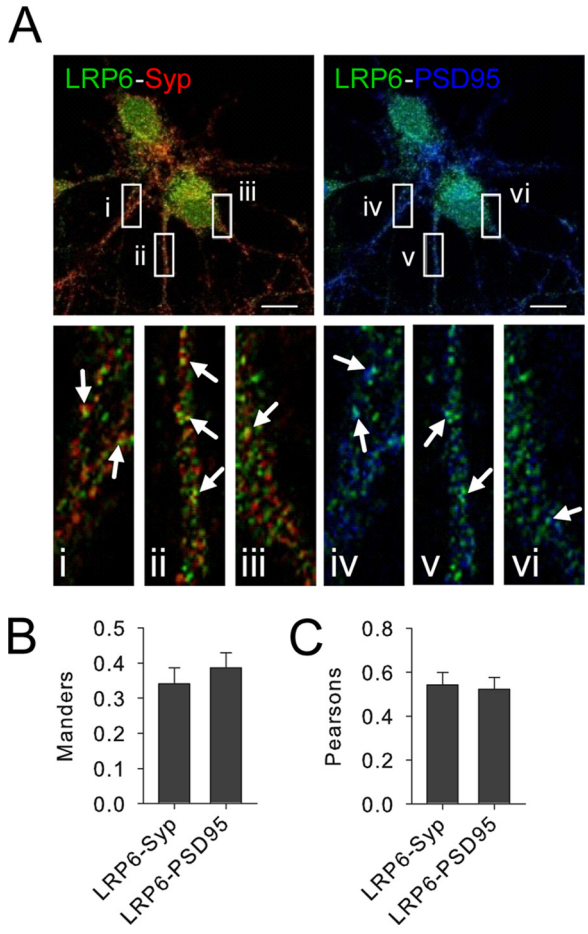

FIGURE 6. **LRP6 immunoreactivity in the soma and neuronal processes associated with pre- and postsynaptic markers Syp and PSD95.** *A*, confocal images were obtained from neurons of 14–15 DIV using antibodies against LRP6 (*green*, Alexa488), Syp (*red*, Cy3), and PSD95 (*blue*, Alexa633). The *arrows* show LRP6-Syp and LRP6-PSD95 colocalization. *Calibration bars*, 20 μm. *B* and *C*, Mander's and Pearson's correlation coefficients for the colocalization of the LRP6 and pre- and postsynaptic markers Syp and PSD95, respectively. The averages of coefficients of at least three regions of interest of 10 neurons were examined.

the effect of purified Wnt3a as excitatory and not inhibitory and further implicated AMPA receptors as the main effectors controlling the action of the Wnt3a protein at the synapse (Fig. 3, *D–F*).

It is well known that synaptic transmission is affected by changes in the presynaptic Ca^{2+} level (31). Notably, the Wnt3a effect on neurotransmission seems to be mediated through a fast influx of Ca^{2+}, which subsequently induced the phosphorylation of Synapsin I and the release of synaptic vesicles from the presynaptic terminal (Fig. 4). Interestingly, the source of this Ca^{2+} influx appeared to be mainly extracellular. Indeed, the Wnt3a effect was nearly abolished when using an external solution with zero nominal calcium and silenced in experiments in the presence of Cd^{2+}, suggesting that influx through voltage-dependent Ca^{2+} channels or transient receptor potential ion channels, which are both Cd^{2+}-sensitive (35–37), could be involved in the Wnt3a-evoked effect. Supporting this idea, it has been recently observed that a Wnt/Ca^{2+} pathway ligand, the Wnt5a protein (19, 20), modulates cortical axonal guidance/repulsion processes via augmenting the concentration of intracellular Ca^{2+} through activation of transient receptor potential ion channels (38). Nevertheless, activation of presynaptic neurotransmitter receptors that are permeable to Ca^{2+} and that enable a sufficient rise in intracellular Ca^{2+} to trigger neurotransmitter release should also be examined in further detail when explaining the remaining 12% in the fluorescent signal associated with the Wnt3a effect in the presence of Cd^{2+} (Fig. 4*B*).

The data, which suggest that cross-talk between Wnt/β-catenin and Wnt/Ca^{2+} signaling could take place in central neurons, are further supported by the following observations. First, we have shown here that purified Wnt3a protein, which is strongly expressed in the hippocampus (39), along with inducing the influx of Ca^{2+}, maintains its activity in the canonical pathway in stabilizing β-catenin and activating a Wnt/β-catenin luciferase-associated gene reporter (Fig. 1) (21, 22). Second, it has been observed that in the proliferation of PC12 cells, the canonical Wnt1 protein activates intracellular components of the Wnt/Ca^{2+} pathway, including the protein kinase C enzyme (40), which has been previously involved in the regulation of neurotransmitter release (41, 42). Third, the Wnt-responsive Dvl (Dishevelled) protein, which acts as a branching point between canonical and noncanonical Wnt signaling pathways, binds to synaptotagmin and thus participates in the process of endo- and exocytosis of neurotransmitter-containing vesicles in differentiated PC12 cells (43). Fourth, the canonical LRP6 coreceptor, which we have previously found expressed in the human hippocampus and genetically linked to prevalent neurological conditions (25), is seen here localized within pre- and postsynaptic regions (Fig. 6), being essential for inducing the intracellular increase of Ca^{2+} to trigger the Wnt3a-dependent effect on neurotransmission (Fig. 5).

Finally, the experimental data reported in this study do not necessarily imply that the Wnt3a effect on neurotransmission would be independent of the activity mediated by β-catenin T cell factor/lymphoid enhancer factor complexes, which have been previously involved in long term potentiation events (16, 18), but rather suggest that such a rapid effect on the neuronal network (*i.e.* min) involves the cross-talk between receptors and kinases acting as canonical or Wnt/Ca^{2+} components, which is the molecular machinery associated with or immediately downstream of its complex receptor at the membrane in the Wnt3a effect on synaptic transmission in mature hippocampal neurons.

Acknowledgments—We acknowledge the efforts of M. Cuevas, J. Fuentealba, and P. Cardenas in the initial steps of this study.

REFERENCES

1. Grove, E. A., Tole, S., Limon, J., Yip, L., and Ragsdale, C. W. (1998) *Development* **125,** 2315–2325
2. Houart, C., Caneparo, L., Heisenberg, C., Barth, K., Take-Uchi, M., and Wilson, S. (2002) *Neuron* **35,** 255–265
3. Lee, S. M., Tole, S., Grove, E., and McMahon, A. P. (2000) *Development* **127,** 457–467
4. Maretto, S., Cordenonsi, M., Dupont, S., Braghetta, P., Broccoli, V., Hassan, A. B., Volpin, D., Bressan, G. M., and Piccolo, S. (2003) *Proc. Natl. Acad. Sci. U.S.A.* **100,** 3299–3304
5. Zhou, C. J., Zhao, C., and Pleasure, S. J. (2004) *J. Neurosci.* **24,** 121–126

6. Lie, D. C., Colamarino, S. A., Song, H. J., Désiré, L., Mira, H., Consiglio, A., Lein, E. S., Jessberger, S., Lansford, H., Dearie, A. R., and Gage, F. H. (2005) *Nature* **437,** 1370–1375
7. Takeichi, M., and Abe, K. (2005) *Trends Cell Biol.* **15,** 216–221
8. Bamji, S. X., Shimazu, K., Kimes, N., Huelsken, J., Birchmeier, W., Lu, B., and Reichardt, L. F. (2003) *Neuron* **40,** 719–731
9. Ciani, L., and Salinas, P. C. (2005) *Nat. Rev. Neurosci.* **6,** 351–362
10. Farías, G. G., Vallés, A. S., Colombres, M., Godoy, J. A., Toledo, E. M., Lukas, R. J., Barrantes, F. J., and Inestrosa, N. C. (2007) *J. Neurosci.* **27,** 5313–5325
11. Hall, A. C., Lucas, F. R., and Salinas, P. C. (2000) *Cell* **100,** 525–535
12. Packard, M., Koo, E. S., Gorczyca, M., Sharpe, J., Cumberledge, S., and Budnik, V. (2002) *Cell* **111,** 319–330
13. Speese, S. D., and Budnik, V. (2007) *Trends Neurosci.* **30,** 268–275
14. Wang, J., Jing, Z., Zhang, L., Zhou, G., Braun, J., Yao, Y., and Wang, Z. Z. (2003) *Nat. Neurosci.* **6,** 1017–1018
15. Ahmad-Annuar, A., Ciani, L., Simeonidis, I., Herreros, J., Fredj, N. B., Rosso, S. B., Hall, A., Brickley, S., and Salinas, P. C. (2006) *J. Cell Biol.* **174,** 127–139
16. Beaumont, V., Thompson, S. A., Choudhry, F., Nuthall, H., Glantschnig, H., Lipfert, L., David, G. R., Swain, C. J., McAllister, G., and Munoz-Sanjuan, I. (2007) *Mol. Cell Neurosci.* **35,** 513–524
17. Cerpa, W., Godoy, J. A., Alfaro, I., Farías, G. G., Metcalfe, M. J., Fuentealba, R., Bonansco, C., and Inestrosa, N. C. (2008) *J. Biol. Chem.* **283,** 5918–5927
18. Chen, J., Park, C. S., and Tang, S. J. (2006) *J. Biol. Chem.* **281,** 11910–11916
19. Kohn, A. D., and Moon, R. T. (2005) *Cell Calcium* **38,** 439–446
20. Slusarski, D. C., Yang-Snyder, J., Busa, W. B., and Moon, R. T. (1997) *Dev. Biol.* **182,** 114–120
21. Willert, K., Brown, J. D., Danenberg, E., Duncan, A. W., Weissman, I. L., Reya, T., Yates, J. R., 3rd, and Nusse, R. (2003) *Nature* **423,** 448–452
22. Kishida, S., Yamamoto, H., and Kikuchi, A. (2004) *Mol. Cell. Biol.* **24,** 4487–4501
23. Aguayo, L. G., and Pancetti, F. C. (1994) *J. Pharmacol. Exp. Ther.* **270,** 61–69
24. Biechele, T. L., and Moon, R. T. (2008) *Methods Mol. Biol.* **468,** 99–110
25. De Ferrari, G. V., Papassotiropoulos, A., Biechele, T., Wavrant De-Vrieze, F., Avila, M. E., Major, M. B., Myers, A., Sáez, K., Henríquez, J. P., Zhao, A., Wollmer, M. A., Nitsch, R. M., Hock, C., Morris, C. M., Hardy, J., and Moon, R. T. (2007) *Proc. Natl. Acad. Sci. U.S.A.* **104,** 9434–9439
26. Carrasco, M. A., Castro, P., Sepulveda, F. J., Tapia, J. C., Gatica, K., Davis, M. I., and Aguayo, L. G. (2007) *Neuroscience* **145,** 484–494
27. Carrasco, M. A., Castro, P. A., Sepulveda, F. J., Cuevas, M., Tapia, J. C., Izaurieta, P., van Zundert, B., and Aguayo, L. G. (2007) *J. Neurochem.* **100,** 1143–1154
28. Gu, X., Olson, E. C., and Spitzer, N. C. (1994) *J. Neurosci.* **14,** 6325–6335
29. Manders, E. M., Verbeek, F. J., and Alen, J. A. (1993) *J. Microsc.* **169,** 375–382
30. Becherer, U., Moser, T., Stühmer, W., and Oheim, M. (2003) *Nat. Neurosci.* **6,** 846–853
31. Sudhof, T. C. (2004) *Annu. Rev. Neurosci.* **27,** 509–547
32. Moon, R. T., Kohn, A. D., De Ferrari, G. V., and Kaykas, A. (2004) *Nat. Rev. Genet* **5,** 691–701
33. Mikels, A. J., and Nusse, R. (2006) *PLoS biology* **4,** e115
34. Arnold, F. J., Hofmann, F., Bengtson, C. P., Wittmann, M., Vanhoutte, P., and Bading, H. (2005) *J. Physiol.* **564,** 3–19
35. Halabisky, B., Friedman, D., Radojicic, M., and Strowbridge, B. W. (2000) *J. Neurosci.* **20,** 5124–5134
36. Inoue, R., Okada, T., Onoue, H., Hara, Y., Shimizu, S., Naitoh, S., Ito, Y., and Mori, Y. (2001) *Circ. Res.* **88,** 325–332
37. Tai, Y., Feng, S., Ge, R., Du, W., Zhang, X., He, Z., and Wang, Y. (2008) *J. Cell Sci.* **121,** 2301–2307
38. Li, L., Hutchins, B. I., and Kalil, K. (2009) *J. Neurosci.* **29,** 5873–5883
39. Roelink, H. (2000) *Curr. Biol.* **10,** R279–281
40. Spinsanti, P., De Vita, T., Caruso, A., Melchiorri, D., Misasi, R., Caricasole, A., and Nicoletti, F. (2008) *J. Neurochem.* **104,** 1588–1598
41. Pozzi, D., Condliffe, S., Bozzi, Y., Chikhladze, M., Grumelli, C., Proux-Gillardeaux, V., Takahashi, M., Franceschetti, S., Verderio, C., and Matteoli, M. (2008) *Proc. Natl. Acad. Sci. U.S.A.* **105,** 323–328
42. Shimazaki, Y., Nishiki, T., Omori, A., Sekiguchi, M., Kamata, Y., Kozaki, S., and Takahashi, M. (1996) *J. Biol. Chem.* **271,** 14548–14553
43. Kishida, S., Hamao, K., Inoue, M., Hasegawa, M., Matsuura, Y., Mikoshiba, K., Fukuda, M., and Kikuchi, A. (2007) *Genes Cells* **12,** 49–61